Electronic Supplementary Material (ESI) for Nanoscale.

Supplemental Material

Figure S1.

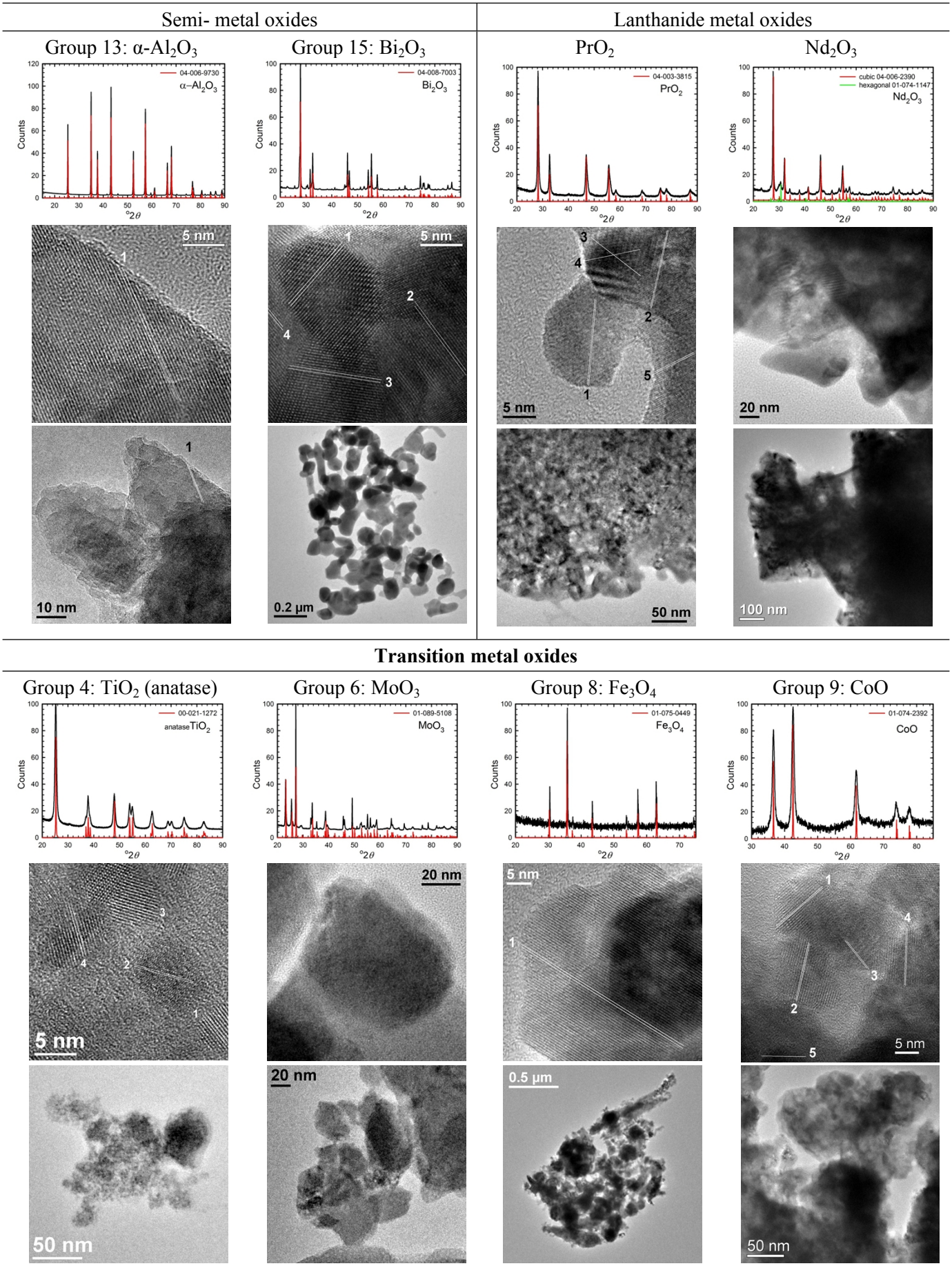
Semi- metal oxides
Lanthanide metal oxides
Group 13: α-Al2O3
Group 15: Bi2O3
PrO2
Nd2O3
04-006-9730
α–Al2O3
04-008-7003
Bi2O3
04-003-3815
PrO2
cubic 04-006-2390
hexagonal 01-074-1147
Nd2O3
Counts
°2θ
5 nm
10 nm
0.2 μm
50 nm
20 nm
100 nm
Transition metal oxides
Group 4: TiO2 (anatase)
Group 6: MoO3
Group 8: Fe3O4
Group 9: CoO
00-021-1272
anatase TiO2
01-089-5108
MoO3
01-075-0449
Fe3O4
01-074-2392
CoO
0.5 μm

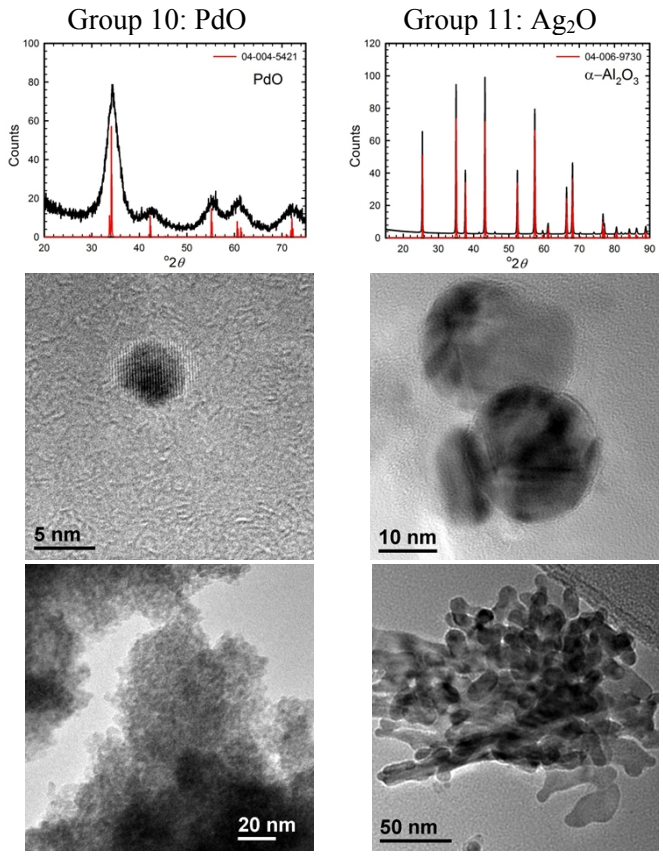

Figure S1. XRD patterns and TEM images of metal oxide nanomaterials synthesized using the solvent-deficient method. The XRD plots show the ICDD standard pattern (red line) matched to the product (black line), with the standard's PDF number given in the legend. The numbered lines in the high-resolution TEM images highlight the lattice fringes whose d-spacings and crystal plane indices are given in Table S2 in the supplemental material.

Table S1. Measured d-spacings (column A) and crystal plane indices (column C) of the highlighted/numbered lattice fringes in the high-resolution TEM images compared to the d-spacings of the standard (column B) matched to each compound in the XRD analyses.

Transition metal oxides					**Semi-metal oxides**				
		A	**B**	**C**			**A**	**B**	**C**
Group 3	Y_2O_3	(1) 3.04 (2) 1.88	3.09 1.89	222 440	Group 13	γ-Al_2O_3	(1) 2.37 (2) 2.37 (3) 2.05	2.28 2.28 1.98	222 $\bar{2}22$ 400
Group 4	TiO_2	(1) 3.52 (2) 2.38 (3) 3.52 (4) 3.51	3.52 2.38 3.52 3.52	101 004 101 101	Group 13	α-Al_2O_3	(1) 3.49	3.49	012
Group 4	ZrO_2	(1) 3.36 (2) 2.66 (3) 3.36	3.36 2.65 3.36	110 101 110	Group 13	In_2O_3	(1) 2.99 (2) 2.99 (3) 2.57 (4) 4.21 (5) 4.21	2.93 2.93 2.54 4.14 4.14	222 222 400 211 211
Group 7	Mn_2O_3	(1) 4.98 (2) 2.77 (3) 4.98	4.71 2.72 4.71	200 222 200	Group 14	SnO_2	(1) 3.36 (2) 2.66 (3) 3.36	3.36 2.65 3.36	110 101 110
Group 8	Fe_2O_3	(1) 2.75 (2) 3.72 (3) 2.22	2.70 3.68 2.21	$10\bar{1}4$ $01\bar{1}2$ $11\bar{2}3$	Group 15	Bi_2O_3	(1) 3.21 (2) 3.21 (3) 3.21 (4) 2.82	3.19 3.19 3.19 2.81	201 201 201 002
Group 8	Fe_3O_4	(1) 4.84	4.82	111	**Lanthanide metal oxides**				
Group 9	CoO	(1) 2.44 (2) 2.45 (3) 2.44 (4) 2.45 (5) 2.13	2.45 2.45 2.45 2.45 2.13	111 111 111 111 200		CeO_2	(1) 3.14 (2) 2.70 (3) 3.16	3.14 2.72 3.14	111 200 111
Group 9	Co_3O_4	(1) 4.69 (2) 2.91 (3) 2.91 (4) 4.69 (5) 4.69	4.67 2.86 2.86 4.67 4.67	111 220 220 111 111		PrO_2	(1) 1.97 (2) 1.97 (3) 1.69 (4) 1.69	1.93 1.93 1.65 1.65	220 220 311 $\bar{3}11$
Group 10	NiO	(1) 2.09 (2) 2.09	2.09 2.09	200 200					
Group 11	CuO	(1) 2.51 (2) 2.34 (3) 2.33	2.53 2.33 2.33	$\bar{1}11$ 111 111					
Group 12	ZnO	(1) 2.53	2.48	$10\bar{1}1$					

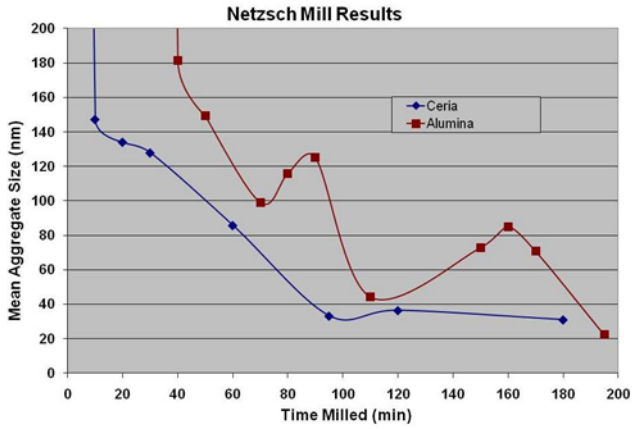

Figure S2. Preliminary Netzsch milling results for the Al_2O_3 (alumina) and CeO_2 (ceria) nanomaterials showing the average agglomerate size as a function of milling time in aqueous solution.

Though the initial sizes (>200nm) of the agglomerates were quite large, the Netzsch mill de-agglomerated both samples easily in water (with the pH controlled to be between 5-6 for the Al_2O_3), resulting in agglomerate sizes of 22 (±15) nm and 31 (±19) nm for the Al_2O_3 and CeO_2 samples, respectively, after only 3 and 1.5 hours of milling, respectively. These agglomerate sizes correspond roughly to five Al_2O_3 and two CeO_2 nanoparticles across, providing additional confirmation that our nanomaterials are soft agglomerates of relatively easily separated nanoparticles, not polycrystalline materials.

Figure S3. XRD patterns/analyses of the dried (D), dried-rinsed-dried (DRD), and rinsed-dried (RD) precursors (where applicable) plotted with the ICDD standard patterns of the materials they contain. The identities and PDF numbers of the standard patterns are given in the legend of each graph.

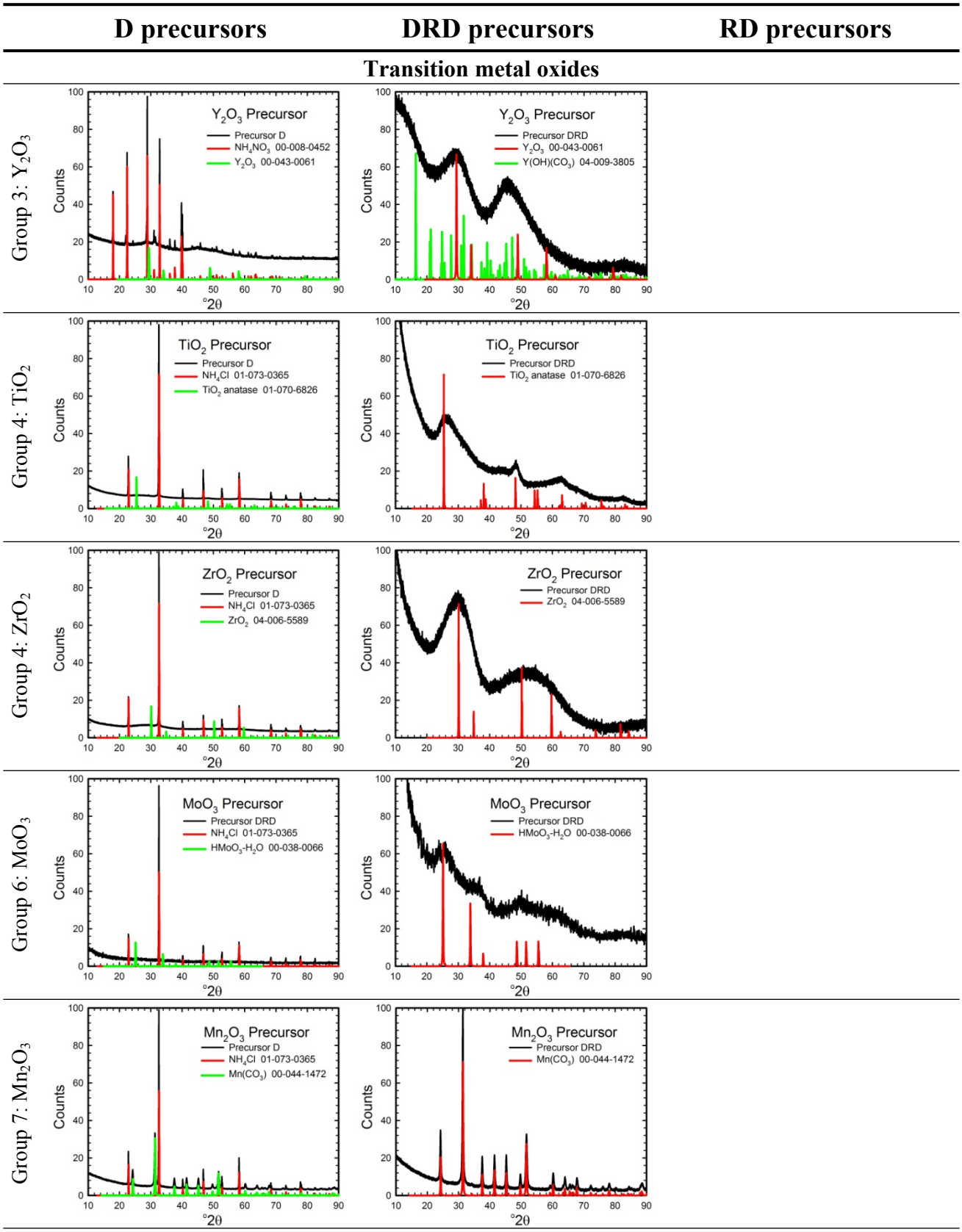

Group 8: Fe_2O_3

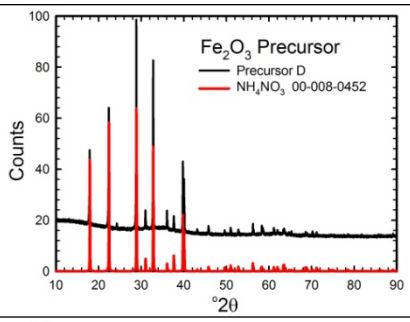

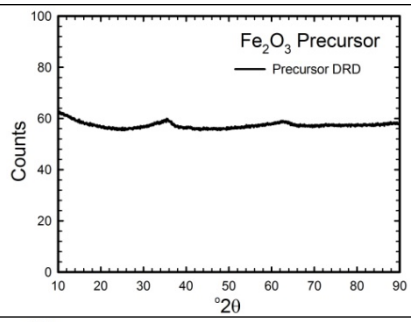

Group 9: CoO

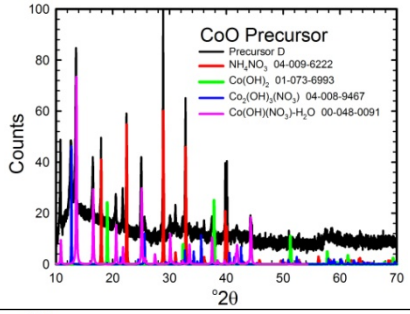

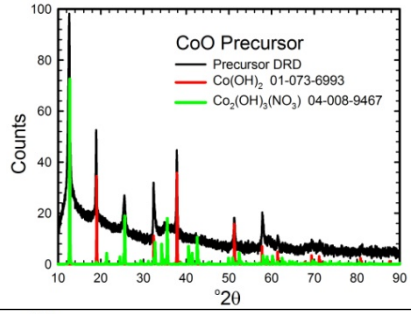

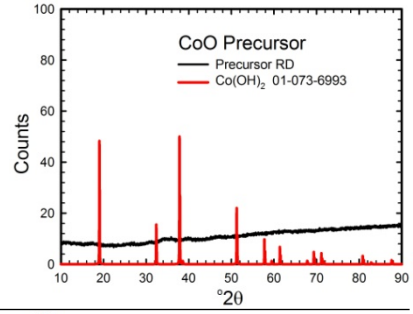

Group 10: NiO

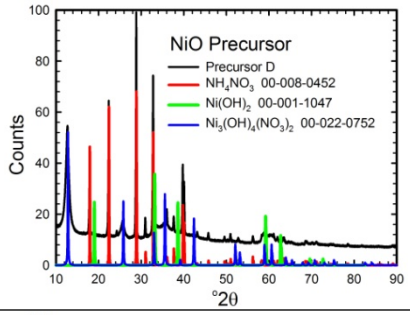

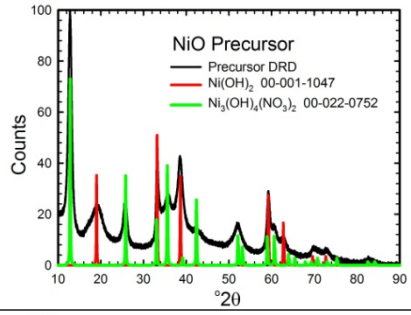

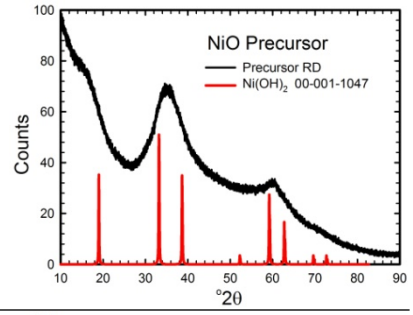

Group 11: CuO

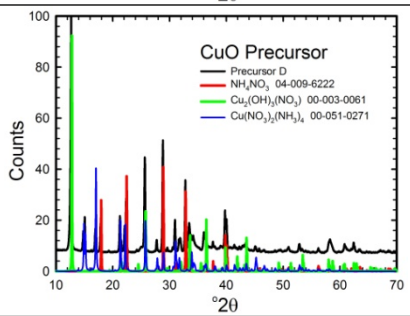

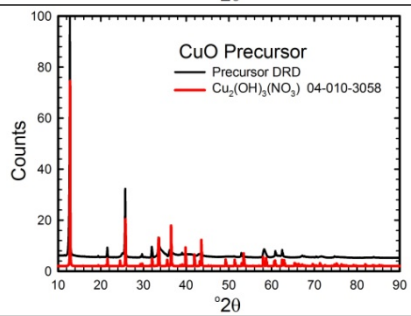

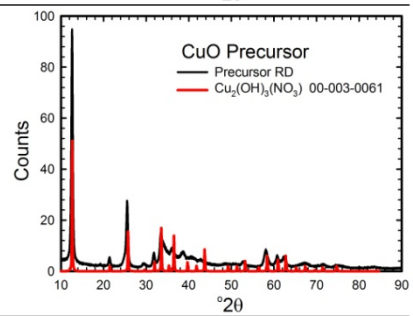

Group 11: Ag_2O

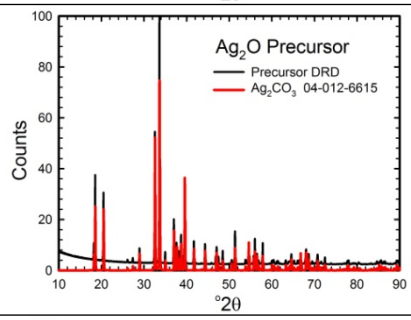

Group 12: ZnO

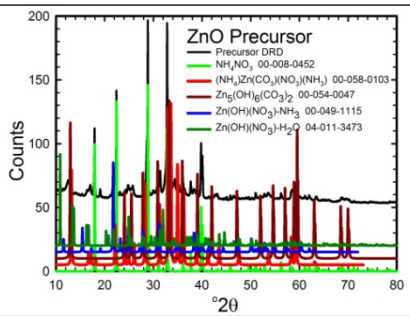

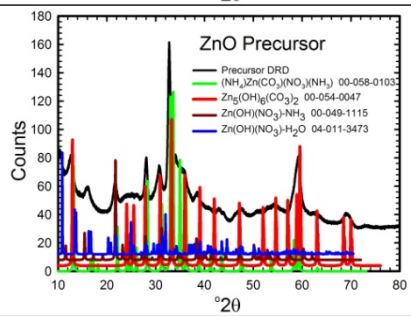

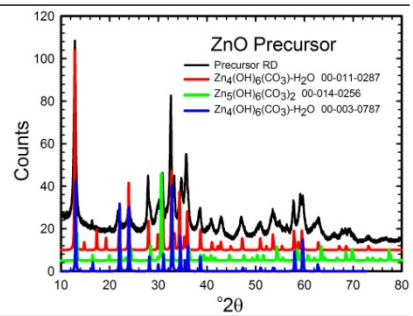

Semi-metal oxides

Group 13: Al_2O_3

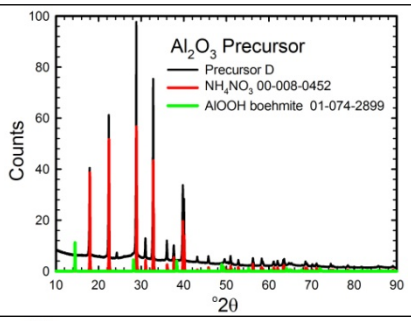

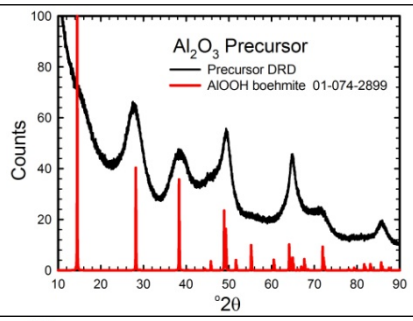

Group 13: In_2O_3

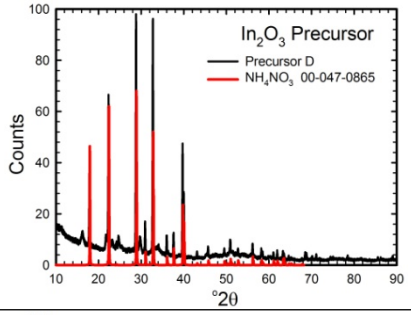

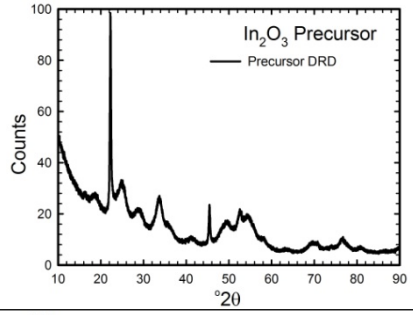

Group 14: SnO_2

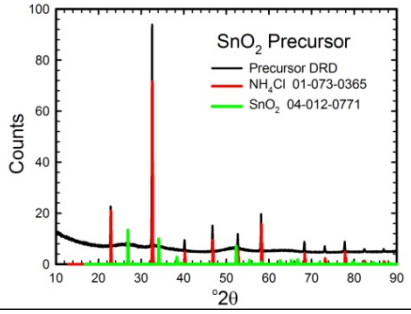

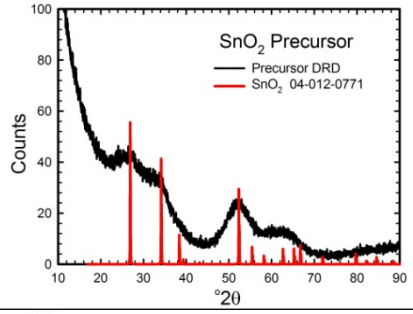

Group 15: Bi_2O_3

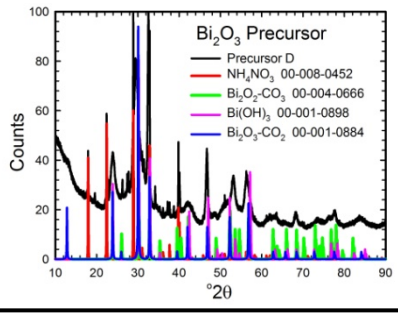

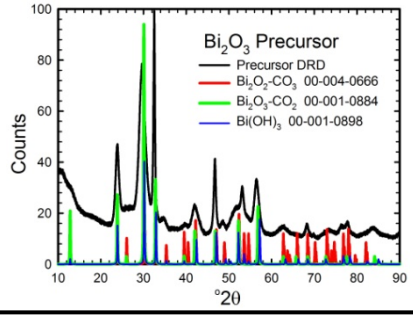

Lanthanide metal oxides

CeO_2

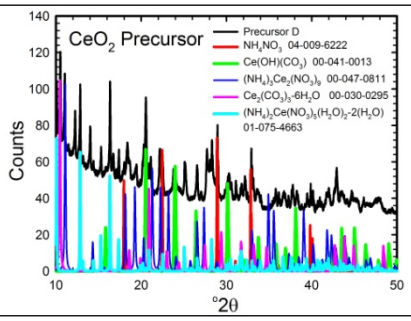

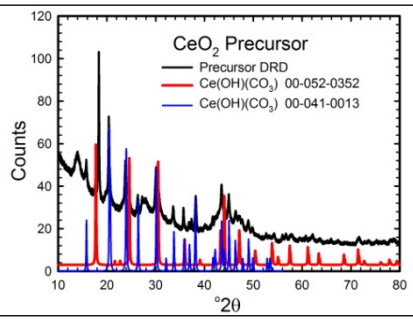

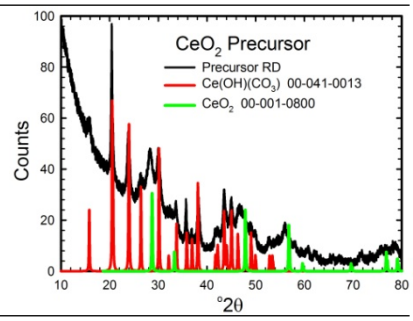

PrO_2	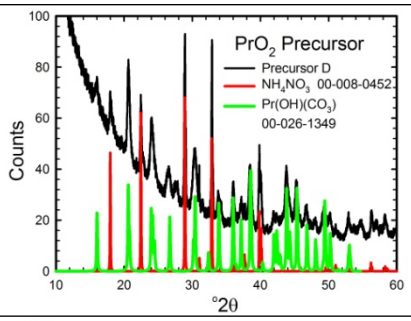 PrO2 Precursor Precursor D NH4NO3 00-008-0452 Pr(OH)(CO3) 00-026-1349 Counts °2θ	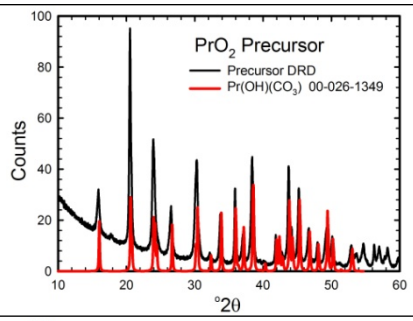 PrO2 Precursor Precursor DRD Pr(OH)(CO3) 00-026-1349 Counts °2θ
Nd_2O_3	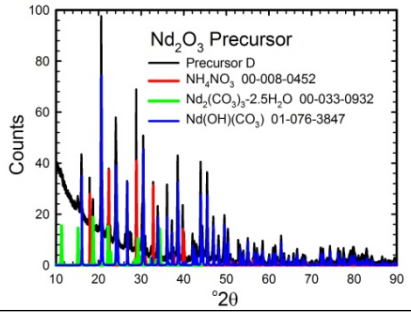 Nd2O3 Precursor Precursor D NH4NO3 00-008-0452 Nd2(CO3)3-2.5H2O 00-033-0932 Nd(OH)(CO3) 01-076-3847 Counts °2θ	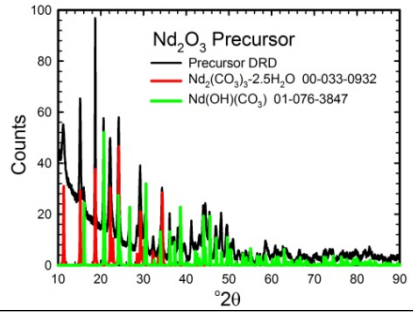 Nd2O3 Precursor Precursor DRD Nd2(CO3)3-2.5H2O 00-033-0932 Nd(OH)(CO3) 01-076-3847 Counts °2θ

Figure S4. TG/DTA-MS data for the dried (un-rinsed) precursors. Positive and negative DTA values correspond to exothermic and endothermic events, respectively.

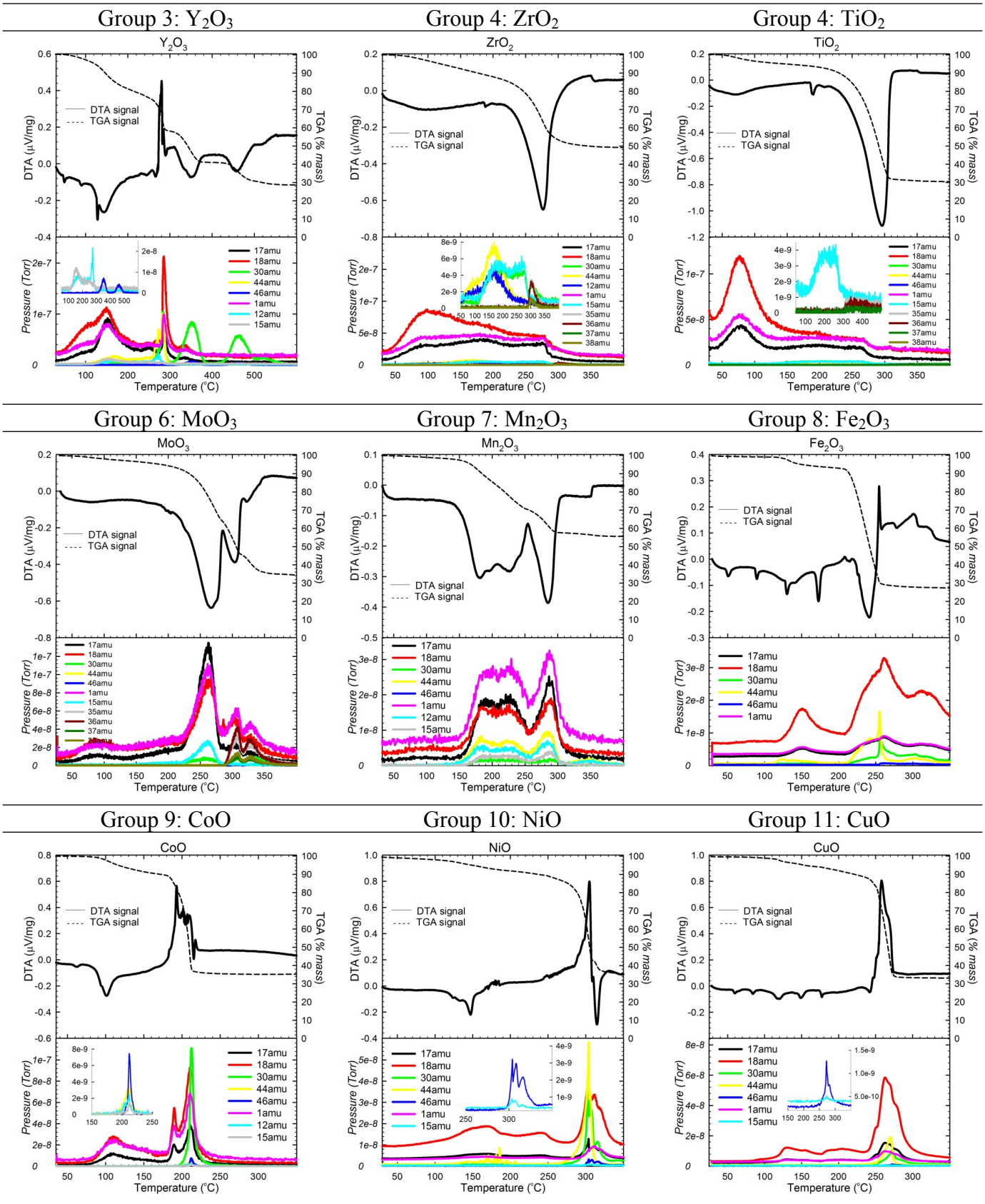

Group 11: Ag_2O

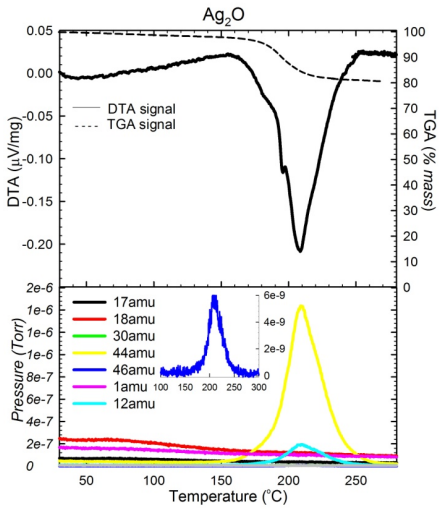

Group 12: ZnO

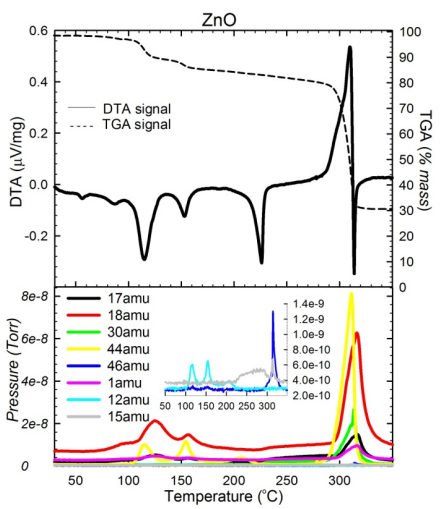

Group 13: Al_2O_3

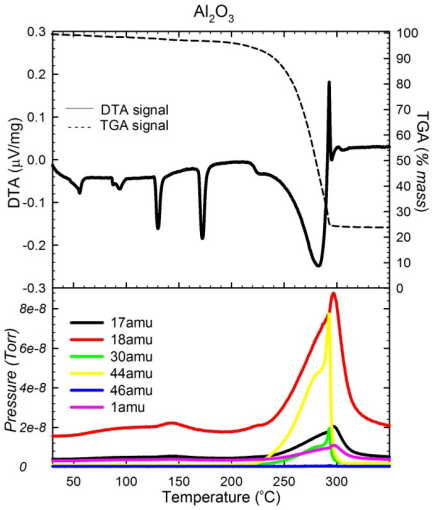

Group 13: In_2O_3

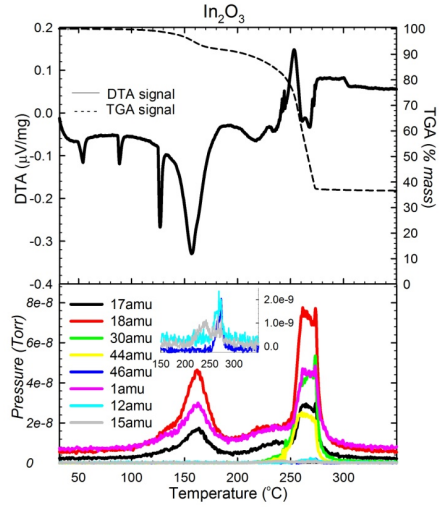

Group 14: SnO_2

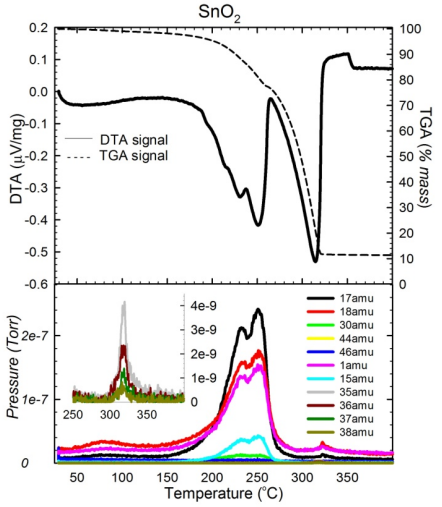

Group 15: Bi_2O_3

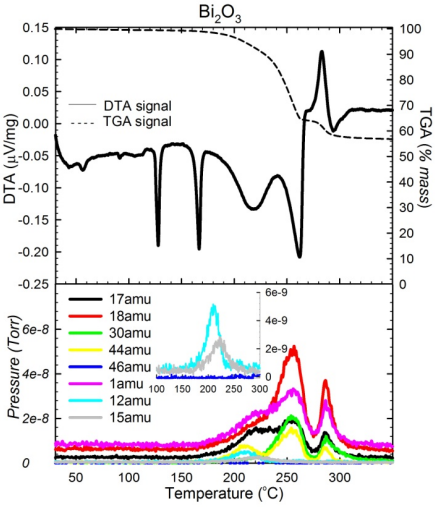

CeO_2

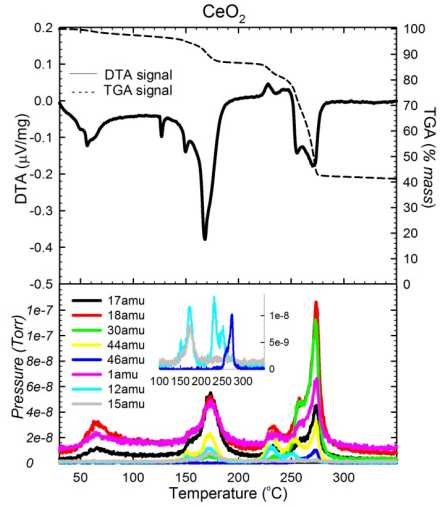

Nd_2O_3

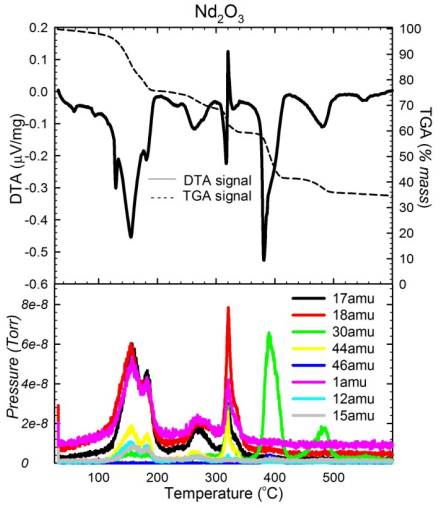

PrO_2

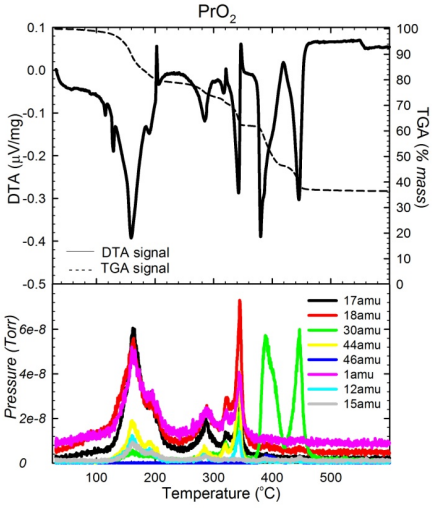

Figure S5. TG/DTA-MS data of the calcination of rinsed precursors.

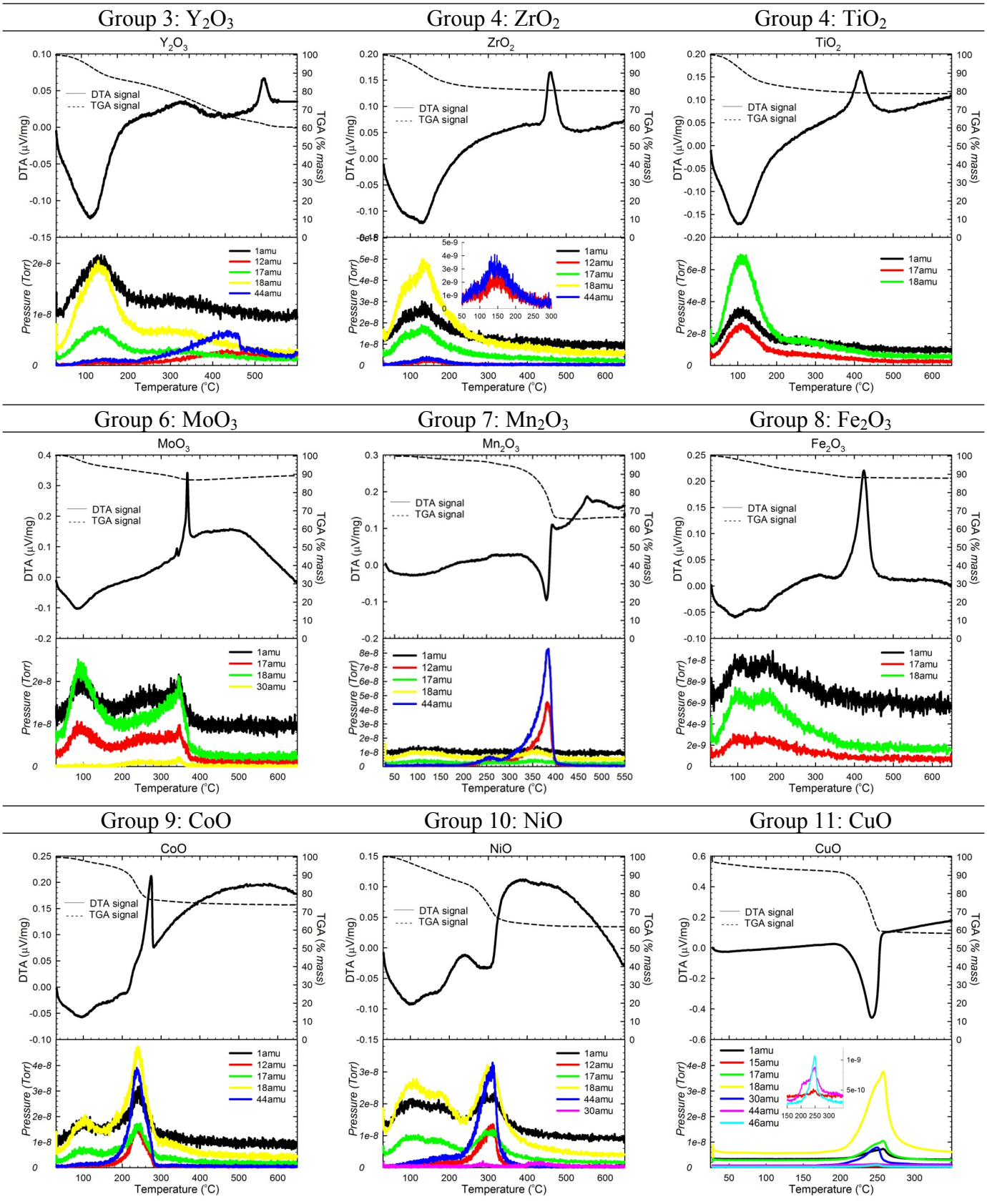

Group 12: ZnO	Group 14: SnO_2	Group 15: Bi_2O_3